G2A Signaling Dampens Colitic Inflammation via Production of IFN- γ

S. Courtney Frasch, Eóin N. McNamee, Douglas Kominsky, Paul Jedlicka, Claudia Jakubzick, Karin Zemski Berry, Matthias Mack, Glenn T. Furuta, James J. Lee, Peter M. Henson, Sean P. Colgan and Donna L. Bratton

---

Supplementary Material   http://www.jimmunol.org/content/suppl/2016/07/08/jimmunol.1600264.DCSupplemental

References   This article **cites 50 articles**, 13 of which you can access for free at:
http://www.jimmunol.org/content/197/4/1425.full#ref-list-1

Why *The JI*? Submit online.

- **Rapid Reviews! 30 days*** from submission to initial decision

- **No Triage!** Every submission reviewed by practicing scientists

- **Fast Publication!** 4 weeks from acceptance to publication

*average

Subscription   Information about subscribing to *The Journal of Immunology* is online at:
http://jimmunol.org/subscription

Permissions   Submit copyright permission requests at:
http://www.aai.org/About/Publications/JI/copyright.html

Email Alerts   Receive free email-alerts when new articles cite this article. Sign up at:
http://jimmunol.org/alerts

G2A Signaling Dampens Colitic Inflammation via Production of IFN-γ

S. Courtney Frasch,* Eóin N. McNamee,[†] Douglas Kominsky,[†,1] Paul Jedlicka,[‡] Claudia Jakubzick,[*,§] Karin Zemski Berry,[¶] Matthias Mack,[‖] Glenn T. Furuta,[#,**] James J. Lee,[††] Peter M. Henson,* Sean P. Colgan,[†,2] and Donna L. Bratton[*,2]

Proinflammatory consequences have been described for lysophosphatidylcholine, a lipid product of cellular injury, signaling via the G protein–coupled receptor G2A on myeloid and lymphoid inflammatory cells. This prompted the hypothesis that genetic deletion of G2A would limit intestinal inflammation in a mouse model of colitis induced by dextran sodium sulfate. Surprisingly, $G2A^{-/-}$ mice exhibited significantly worsened colitis compared with wild-type mice, as demonstrated by disease activity, colon shortening, histology, and elevated IL-6 and IL-5 in colon tissues. Investigation of inflammatory cells recruited to inflamed $G2A^{-/-}$ colons showed significantly more TNF-α^+ and Ly6C^{hi}MHCII$^-$ proinflammatory monocytes and eosinophils than in wild-type colons. Both monocytes and eosinophils were pathogenic as their depletion abolished the excess inflammation in $G2A^{-/-}$ mice. $G2A^{-/-}$ mice also had less IFN-γ in inflamed colon tissues than wild-type mice. Fewer CD4$^+$ lymphocytes were recruited to inflamed $G2A^{-/-}$ colons, and fewer colonic lymphocytes produced IFN-γ upon ex vivo stimulation. Administration of IFN-γ to $G2A^{-/-}$ mice during dextran sodium sulfate exposure abolished the excess colitic inflammation and reduced colonic IL-5 and eosinophil numbers to levels seen in wild-type mice. Furthermore, IFN-γ reduced the numbers of TNF-α^+ monocyte and enhanced their maturation from Ly6C^{hi}MHCII$^-$ to Ly6C^{int}MHCII$^+$. Taken together, the data suggest that G2A signaling serves to dampen intestinal inflammation via the production of IFN-γ, which, in turn, enhances monocyte maturation to a less inflammatory program and ultimately reduces eosinophil-induced injury of colonic tissues. *The Journal of Immunology*, 2016, 197: 1425–1434.

T he inflammatory bowel diseases (IBD), including both ulcerative colitis and Crohn's disease, are debilitating mucosal disorders of unknown etiology (1). The most recent evidence suggests IBD results from an inappropriately directed inflammatory response to the intestinal microbiota in a genetically susceptible host. Epithelial cells are crucial in the maintenance of colonic tissue homeostasis, as IBD is characterized by a breakdown of the intestinal epithelial barrier leading to increased exposure of the mucosal immune system to antigenic luminal material. Because the epithelium functions as the critical interface between the intestinal lumen and the subepithelial mucosa, it is thereby anatomically positioned as a central coordinator of mucosal inflammatory response.

Studies to date indicate that cytokines and chemokines that are produced locally at sites of inflammation play an important role in onset and progression of IBD. IFN-γ, present in IBD, has been shown to have a proinflammatory role in a number of autoimmune and inflammatory diseases (1, 2). The dextran sodium sulfate (DSS) model of murine colitis results from direct epithelial injury, followed by recruitment of inflammatory cells and their inappropriate response to the microflora of the gut (3). The acute phase is characterized by the production of proinflammatory cytokines, including IFN-γ, similar to that observed in human IBD (4–7).

The G protein–coupled receptor, Gpr132 (G2A), is expressed on most leukocytes, for example, lymphocytes, monocytes, and granulocytes [www.immgen.org (8)]. Signaling by G2A is poorly understood and varies widely depending on its activator and the responding cell type and inflammatory context (8). One such stimulant is lysophosphatidylcholine (lysoPC), a lipid produced by injured epithelium, for example, in the airways (9, 10) and colon (11, 12). LysoPC signaling through G2A induces chemotaxis of monocytes, macrophages, and lymphocytes (13–15) and enhances the production of reactive oxygen species by phagocytes (16, 17) and IFN-γ from lymphocytes (18).

Given the observations noted above that G2A signaling heightens inflammatory cell recruitment and host defense responses, we hypothesized that deficiency of G2A, or antagonism of its signaling, would be beneficial in colitis. However, contrary to

*Department of Pediatrics, National Jewish Health, Denver, CO 80206; †Mucosal Inflammation Program, Department of Anesthesiology, University of Colorado, Anschutz Medical Campus, Aurora, CO 80045; ‡Department of Pathology, University of Colorado, Anschutz Medical Campus, Aurora, CO 80045; §Department of Immunology and Microbiology, University of Colorado, Anschutz Medical Campus, Aurora, CO 80206; ¶Department of Pharmacology, University of Colorado Denver, Anschutz Medical Campus, Aurora, CO 80045; ‖Department of Internal Medicine, University of Regensburg, 93042 Regensburg, Germany; #Digestive Health Institute, Children's Hospital Colorado, Aurora, CO 80045; **Gastrointestinal Eosinophilic Diseases Program, Department of Pediatrics, University of Colorado School of Medicine, Aurora, CO 80045; and ††Division of Pulmonary Medicine, Department of Biochemistry and Molecular Biology, Mayo Clinic in Arizona, Scottsdale, AZ 85259

[1]Current address: Department of Microbiology and Immunology, Montana State University, Bozeman, MT.

[2]S.P.C. and D.L.B. contributed equally to this work.

ORCIDs: 0000-0002-3331-3148 (E.N.M.); 0000-0003-1934-8405 (P.M.H.); 0000-0003-0431-8887 (S.P.C.).

our hypothesis, genetic deficiency of G2A resulted in significantly worsened colitis in the knockout (G2A$^{-/-}$) mice compared with wild-type (WT) animals. These data demonstrate that whereas production of lysoPC was similar in both G2A$^{-/-}$ and WT mice during DSS exposure, deficient IFN-γ production within colon tissues of the G2A$^{-/-}$ mice led to worsened injury that was rectified by exogenous administration of IFN-γ. These data support the unexpected conclusion that signaling via the G protein–coupled receptor G2A serves to counterbalance overexuberant innate immune cell injury in DSS colitis via the enhanced production of IFN-γ.

Materials and Methods

Reagents

Anti-CD45 BV510 or allophycocyanin, anti-Ly6C allophycocyanin-Cy7, anti-Ly6G PE, anti-MHCII BV421, anti-CD11b PerCPCy5.5, anti-CD11c PE-Cy7, anti–IFN-γ PE, anti–TNF-α allophycocyanin, anti-CD3 PerCPCy5.5, anti-CD8 PE, anti-CD4 allophycocyanin-Cy7, anti-NKp46 PE-Cy7, and anti-B220 Alexa488 were from BioLegend (San Diego, CA). Anti-CD16/32 (Fc-block), anti-SiglecF PE, and anti-F4/80 Alexa488 were from BD Biosciences (San Diego, CA). Blue fixable Live/Dead was from Invitrogen. Anti-CCR2 (clone MC-21) was provided by M. Mack (University of Regensburg, Regensburg, Germany). Anti–IL-5 (clone TRFK5) was provided by J. Lee (Mayo Clinic, Scottsdale, AZ). Mouse rIFN-γ was from R&D Systems. Collagenase D was from Roche Diagnostics (Indianapolis, IN), and collagenase VIII was from Sigma-Aldrich (St. Louis, MO). The 1-oleoyl-2-hydroxy-*sn*-glycerol-3-phosphocholine (LPC) was from Avanti Polar Lipids (Alabaster, AL).

Mice

Male and female C57BL/6 (WT) mice were purchased from The Jackson Laboratory (Bar Harbor, ME) and were generated from a breeding colony at National Jewish Health (Denver, CO). G2A$^{-/-}$ breeder pairs on a C57BL/6 background were a gift of C. Hedrick (La Jolla Institute for Allergy and Immunology, La Jolla, CA) and were bred in house. All animals received care in accordance with the guidelines of the Institutional Animal Care and Use Committee and were maintained on food and water ad libitum. Mice between the ages of 8 and 12 wk were used and were age and gender matched for all experiments. WT and G2A$^{-/-}$ mice were cohoused for 7–10 d prior to induction of colitis. Preliminary experiments demonstrated that the results following 7-d cohousing were identical to those following 14 d of cohousing.

Induction of colitis and treatments

Experimental colitis was induced in mice by adding 3% (w/v) DSS (m.w. 36,000–50,000; MP Biomedicals, Santa Ana, CA) to drinking water for various numbers of days (2–6 d, as indicated). Fresh DSS solutions were replaced at 3 d. The animals were monitored daily for disease activity using the parameter of weight loss, stool consistency, and fecal blood. Disease activity index was calculated, as described by Cooper et al. (19), as the sum of scores of stool consistency (0 = normal; 1 = near normal; 2 = loose stool; 3 = very loose stool; 4 = diarrhea) and establishment of ulceration of the colon as detected by blood in the feces (0 = negative; 1 = near negative; 2–3 = positive; 4 = gross bleeding) for a maximum score of 8. On the final day, mice were humanely euthanized and colons were harvested. Colon length was measured as an indicator of disease severity. For depletion of monocytes, 20 μg anti-CCR2 (clone MC-21) or isotype control was injected i.p. on consecutive 5 d starting at day 1 after administration of DSS. For depletion of eosinophils, 200 μg anti–IL-5 (clone TRFK5) or isotype control was injected i.p. on consecutive 5 d starting on day 1 after administration of DSS. For IFN-γ restoration experiments, mice received 5 μg mouse rIFN-γ (R&D Systems) i.p. on days 3 and 5 after administration of DSS.

Histology

Sections from the distal colon of each mouse were fixed in 10% formalin before staining with H&E. All histological quantitation was performed blinded by a trained pathologist (P.J.). Colitis severity was determined by three independent parameters, as described previously (20). Severity of inflammation (0–3: none, slight, moderate, severe), extent of injury (0–3: none, mucosal, mucosal and submucosal, transmural), and crypt damage (0–4: none, basal one-third damaged, basal two-thirds damaged, only surface epithelium intact, entire crypt and epithelium lost). The score of each parameter was multiplied by a factor reflecting the percentage of tissue involvement (X1: 0–25%, X2: 26–50%, X3: 51–75%, X4: 76–100%), and all numbers were summed for a total histologic index.

Isolation of colonic lamina propria leukocytes and splenocytes

Colons were opened longitudinally, flushed with PBS to remove contents, and cut into 1-cm pieces. Epithelial cells were depleted by incubation in 15 mL HBSS (Mediatech, Manassas, VA) supplemented with 15 mM HEPES (pH 7.2), 2 mM EDTA and 2% heat-inactivated FBS (Atlanta Biologicals, Lawrenceville, GA), 100 μg/ml streptomycin, and 100 U/ml penicillin at 37°C for 40 min with constant shaking. The epithelial cell–depleted colon tissue was washed in PBS to remove the EDTA, minced, and digested in 10 mL RPMI 1640 supplemented with 15 mM HEPES (pH 7.2), 5% heat-inactivated FBS (Atlanta Biologicals, Lawrenceville, GA), 2 mM L-glutamine, 100 μg/ml streptomycin, 100 U/ml penicillin, 1.2 mg/ml collagenase D, and 0.85 mg/ml collagenase VIII for 30 min at 37°C with constant shaking. Digested colon cells were passed through a 100-μm filter to remove undigested tissue, and the cells were centrifuged at 200 × g for 10 min. Total cells from colon digests were determined by coulter counts, and cells were either cultured ex vivo or stained for analysis by flow cytometry (see below).

After the spleen was harvested from untreated mice, a single-cell suspension was obtained by manually disrupting spleens through a 70-μm cell strainer (BD Falcon, Bedford, MA) with HBSS. Following lysis of RBCs, the splenocytes were refiltered with a 40-μm cell strainer and resuspended at 2.5 × 10^6 cells/ml in RPMI 1640 supplemented with 15 mM HEPES (pH 7.2), 0.1% BSA, 2 mM L-glutamine, 100 μg streptomycin, and 100 U/ml penicillin and stimulated, as described below.

Flow cytometry

Isolated lamina propria cells were incubated with Fc block and stained with Abs, and flow cytometry was performed on a BD LSRII or BD LSRFortessa. Data were analyzed on FlowJo X v.10.0.7 (Tree Star). See Supplemental Fig. 1 for gating strategy. Briefly, immune cell subsets were identified among live CD45$^+$ cells after doublet exclusion.

For determination of colonic tissue or colonic vascular localization of lamina propria leukocytes, 5 μl anti-CD45 allophycocyanin in 200 μl PBS was injected i.v. 5 min before euthanasia. This method allows for the differential identification of cells that are extravascular (at least excluded from Ab labeling) and most likely located within the colonic tissue versus cells that are within the colonic vascular lumen. Total cell subsets were determined by multiplying the percentage of the cell subset, as determined by flow cytometry, by the total cell counts.

Culture and stimulation of colon tissue digests and spleen cells

For culture ex vivo, 1 × 10^6 digested colon cells in 200 μl RPMI 1640 supplemented with 10% heat-inactivated FBS (Atlanta Biologicals, Lawrenceville, GA), 15 mM HEPES (pH 7.4), 2 mM L-glutamine, 100 μg/ml streptomycin, and 100 U/ml penicillin were left unstimulated or stimulated with 1× cell stimulation mixture (PMA plus ionomycin; eBioscience, San Diego, CA) in the presence or absence of 1× protein transport inhibitor (brefeldin A and monensin; eBioscience) for 4 h at 37°C. Cell-free supernatants were analyzed for IFN-γ or TNF-α by ELISA (ELISA Tech, Aurora, CO). Cells treated with protein transport inhibitor were stained for surface markers, fixed, and permeabilized with the Fox P3 permeabilization kit (eBioscience), according to the manufacturer's instructions for intracellular staining of IFN-γ and TNF-α. For ex vivo stimulation of naive spleen cells, 0.5 × 10^6 spleen cells in 200 μl RPMI 1640 supplemented with 0.1% BSA, 15 mM HEPES (pH 7.4), 2 mM L-glutamine, 100 μg/ml streptomycin, and 100 U/ml penicillin were left unstimulated or stimulated with 0.5× stimulation mixture in the absence or presence of 10 μM LPC. A 10× stock of LPC was made by drying the LPC under a flow of nitrogen in a glass tube and resuspending in RPMI 1640 supplemented with 0.1% BSA. LPC was dissolved by sonication in a water bath sonicator. LPC was added simultaneously with the stimulation mixture. Cell-free supernatants were analyzed for IFN-γ by ELISA (ELISA Tech).

Cytokine determinations

Proinflammatory cytokines were measured by using the MesoScale Discovery Platform (Proinflammatory Panel 1; MSD, Rockford, MD) in serum obtained following cardiac puncture or homogenates from sections of distal colon, according to the manufacturer's instructions.

Quantitative PCR

Sections from distal colon were snap frozen and stored at −80°C. Total RNA was isolated using the Qiagen mini RNA isolation kit, according to the manufacturer's instructions, and reverse transcribed using iScript cDNA Synthesis Kit (Bio-Rad, Hercules, CA). Real-time quantitative PCR was performed, and data were normalized to *GusB* and calculated as relative quantity ($2^{-\Delta\Delta Ct}$, where Ct is cycle threshold for each sample). The indicated forward and reverse primer pairs were purchased from Bio-Rad.

Lysophospholipid measurement

Colon tissues were collected, weighed, and homogenized in MeOH/water (50:50). Lysophosphatidylcholine (lysoPC) internal standard (17:1/OH-phosphatidylcholine) was added, and total lipids were extracted by the method of Bligh and Dyer (21). The organic layer was collected and brought to dryness. Phospholipid classes were separated by application to an aminopropyl SepPak (NH2-DSC) column, and lysoPC was eluted with MeOH. LysoPC was measured in positive ion mode by precursors of m/z 184 by liquid chromatography–tandem mass spectrometry, as previously described (22). For lysophosphatidylserine (lysoPS) measurements, colon tissues were collected, weighed, minced, and extracted in MeOH. LysoPS internal standard (17:1/OH-phosphatidylserine) was added, and insoluble material was centrifuged at $10,000 \times g$ for 10 min. The MeOH supernatant was applied to an aminopropyl SepPac (NH2-DSC) column to separate lipid classes, and lysoPS was eluted in ammonium hydroxide:MeOH 10:90 (v/v). LysoPS species were monitored by multiple reaction monitoring by LC-MS/MS in negative ion mode, as described previously (23).

Statistical analysis

Data are presented as the means ± SEM. Data represent three to five mice per group and at least two independent experiments, unless otherwise stated. Unpaired *t* test and one-way or two-way ANOVA test were used to determine differences between groups, as indicated, where $p < 0.05$ was considered significant (GraphPad Prism, La Jolla, CA).

Results

G2A deficiency does not alter intestinal homeostasis, but results in worsened DSS-induced colitis

Initial studies confirmed the lack of intrinsic intestinal inflammation in naive mice globally deficient for G2A. Histologic examination of colonic tissues showed no epithelial disruption or obvious inflammation in either $G2A^{-/-}$ or WT mice at baseline (Supplemental Fig. 1A). Colon lengths and lysoPC levels were no different between the two genotypes in the naive state (Supplemental Fig. 1B, 1C). $CD45^+$ cells in digests of colonic tissues were examined by flow cytometry (see gating strategy in Supplemental Fig. 1D). There were no baseline differences between the genotypes with regard to total numbers of macrophages, monocytes, eosinophils, neutrophils, or lymphocytes (data not shown). As expected, G2A was expressed in the $CD45^+$ cells from WT colons, but not from the $G2A^{-/-}$ colons, whereas isolated colonic epithelial cells were negative for G2A expression in both genotypes (data not shown). Total colon tissue was also analyzed by quantitative PCR for proinflammatory cytokines, TNF-α, IL-6, IL-1β, IFN-γ, IL-12p70, IL-4, IL-13, and IL-5. Expression levels were very low or undetectable, and no significant differences were noted between the genotypes (data not shown).

In a well-described intestinal inflammation model (3, 4), DSS (3%) was added to drinking water of both $G2A^{-/-}$ and WT mice and continued for 6 d. Disease activity was calculated using the parameters of stool consistency and fecal blood, which were determined daily for each mouse, as described in experimental procedures, with a maximum of 8 points (19). By day 3, disease activity was evident in some mice of both genotypes and became more severe with increasing duration of DSS exposure (Fig. 1A). Over the time course of DSS exposure, $G2A^{-/-}$ mice had significantly greater disease activity scores than WT mice, and by day 6, had overt diarrhea and bleeding into the stool. By day 6, most $G2A^{-/-}$ mice had reached criteria to be euthanized. $G2A^{-/-}$ mice tended to lose more weight over the course of DSS exposure than WT mice. On sacrifice at day 6, colon length was measured and found to be significantly shorter in $G2A^{-/-}$ mice than WT animals (Fig. 1B). Histologic examination of colonic tissues at day 6 showed marked inflammatory infiltrates in both genotypes and almost complete loss of crypt architecture in the distal colons of the $G2A^{-/-}$ mice (Fig. 1C). Accordingly, blinded histologic scoring of colonic tissues was significantly worse for $G2A^{-/-}$ mice than for WT mice.
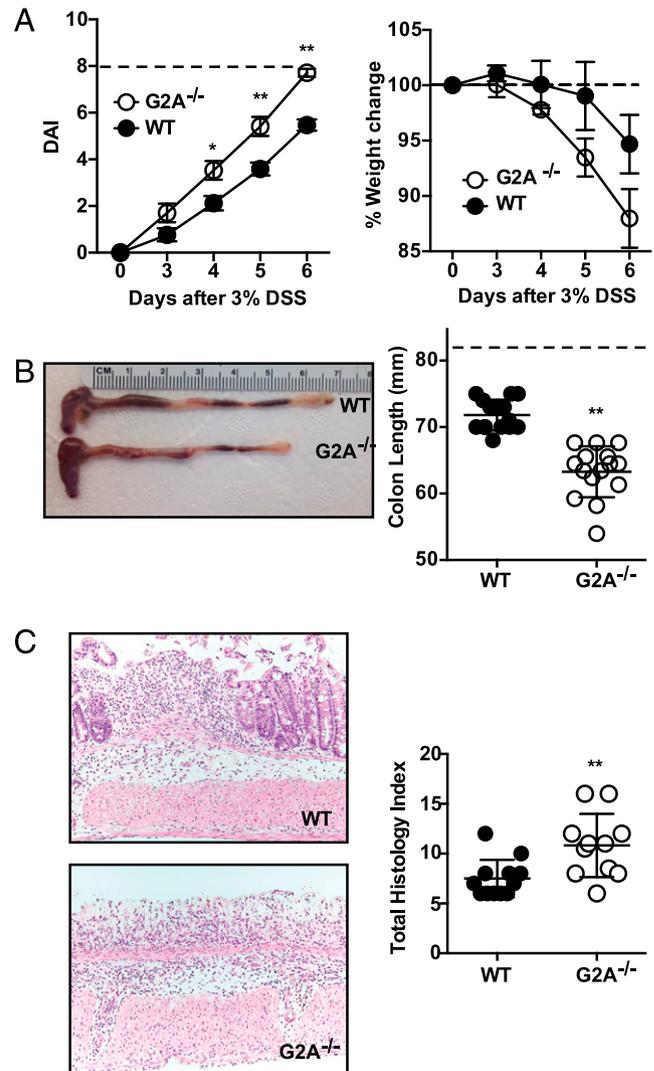
FIGURE 1. Loss of G2A receptor signaling exacerbates DSS-induced colitis. (**A**) Disease activity (DAI) (left) and percentage of change in weight (right) were determined daily during DSS administration, as described in *Materials and Methods*. Dotted line indicates maximum DAI score (left) or initial body weight at day 0 (right). (**B**) Colon length as a measure of disease severity was determined on day 6 after 3% DSS administration. Left, Representative photograph of WT and $G2A^{-/-}$ colons. Right, Summated colon lengths for each genotype. Dotted line represents colon length of water control animals (see Supplemental Fig. 1B). (**C**) Left, Representative histologic images of the distal colon on day 6 (original magnification ×10). Right, Quantitative total histologic index. Data represent mean ± SEM, $n = 15$. *$p < 0.05$, **$p < 0.01$ versus WT.

Recruited inflammatory cells ($CD45^+$) were analyzed by flow cytometry (Supplemental Fig. 1E gating strategy) following digestion of the total colonic tissue. In DSS-induced colitis, monocytes are a prominent recruited inflammatory cell and are thought to be largely responsible for orchestrating responses to commensal microbes that result in further colonic injury (24–27). We found monocyte numbers to be increased in both genotypes over time of DSS administration, but were significantly more numerous in the $G2A^{-/-}$ mice by day 6 (Fig. 2A). Because signaling via G2A has been shown to mediate chemotaxis of inflammatory cells, including monocytes (8, 13), it was important to determine whether the monocytes within the colons were similarly distributed in the tissues versus vasculature in the two genotypes. To this end, mice were injected i.v. with anti-CD45 just prior to sacrifice to separately tag cells in the colonic intravascular com-
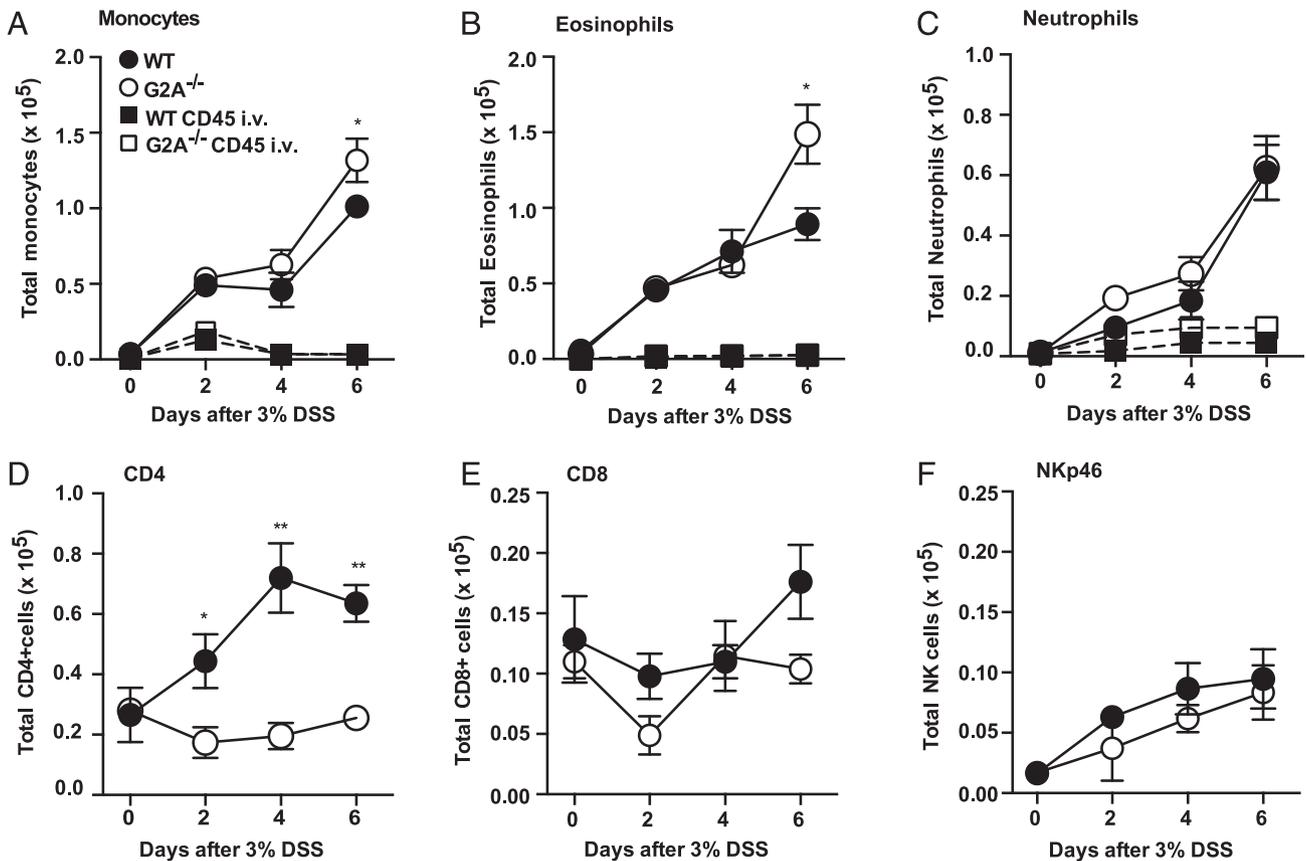
FIGURE 2. G2A$^{-/-}$ mice show altered recruitment of immune cells over the course of DSS-induced colitis. (**A–F**) Immune cell types were determined by flow cytometry following digestion, as described in *Materials and Methods*. Gating strategy is described in *Materials and Methods* and Supplemental Fig. 1E. Note differences in scale. Square symbols denote myeloid cells tagged with i.v. anti-CD45 (see *Materials and Methods*). Data represent mean ± SEM, $n = 8$–10. $*p < 0.05$, $**p < 0.01$ compared with WT.

partment and thereby providing a snapshot of cells present in this compartment. As shown in Fig. 2A, intravascular monocytes (those labeling with anti-CD45) peaked at day 2 in both genotypes and appeared to be equivalent. For the most part, monocytes were extravascular (or sequestered from the Ab) in the inflamed colons of both genotypes, demonstrating no obvious deficiency in recruitment of monocytes or distribution in colonic tissues in G2A$^{-/-}$ mice during DSS colitis. Eosinophils in colonic tissues during DSS colitis mirrored monocytes (Fig. 2B). Their numbers rose over the first 4 d of colitis similarly in both genotypes with few appearing to be intravascular by anti-CD45 labeling. However, significantly more eosinophils were present in the colons of G2A$^{-/-}$ mice by day 6. Recruited neutrophils were much fewer than monocytes and eosinophils, and no differences between the genotypes were evident (Fig. 2C). Unlike the other myeloid cell types, intravascular neutrophils constituted a substantial proportion of total neutrophils, ~25–30% on days 2–4 of DSS exposure, in both genotypes.

Although DSS-induced colitis develops independently of lymphocytes in Rag$^{-/-}$ mice (28), we did assess the lymphocyte populations in the inflamed colons. A population of CD4 cells was recruited to the colons of WT mice, but was strikingly deficient in the colons of G2A$^{-/-}$ mice throughout DSS exposure (Fig. 2D). CD8 cells were present in colons of both genotypes, and no differences in numbers were detected (Fig. 2E). NK cells (Fig. 2F) and B cells (data not shown) were also recruited to inflamed colons in similar numbers for both genotypes.

Colon tissues were assessed for several proinflammatory cytokines and mediators reportedly produced during the acute-phase

DSS-induced colitis (4–7). Inflamed colon tissues harvested on day 6 from G2A$^{-/-}$ mice demonstrated significantly higher amounts of IL-6 and IL-5 in comparison with WT (Fig. 3A). In contrast, IFN-γ levels in colon tissue were much lower in G2A$^{-/-}$ mice (Fig. 3B). No differences between the genotypes were seen for colon tissue levels of TNF-α, IL-12p70, IL-1β, CXCL1, or IL-10 (data not shown). Message for CCL5, CCL11, CCL24, IL-13, and IL-4 was determined by quantitative PCR, with no differences detected between the genotypes (data not shown). LysoPC, associated with injury of epithelium (11, 12), was also measured in colonic tissues from both genotypes over time. Importantly, LysoPC levels were elevated over baseline and appeared to peak at day 4 of DSS exposure, but were no different between the genotypes (Fig. 3C).

In summary, the G2A$^{-/-}$ mice, relative to WT mice, showed significantly worsened disease on all measures, and showed increased numbers of monocytes and eosinophils and fewer CD4 lymphocytes recruited to injured colons than WT mice. Differences in cytokines present in colon tissues appeared to be elevated IL-6 and IL-5, and diminished IFN-γ in the G2A$^{-/-}$ mice relative to WT.

Worsened colitis in G2A-deficient mice is driven by proinflammatory monocytes in an eosinophil-dependent manner

Earlier studies from several groups have shown that monocyte populations infiltrating the inflamed colon exhibit marked heterogeneity, with transition over time from a so-called proinflammatory phenotype to an anti-inflammatory phenotype (26, 27).
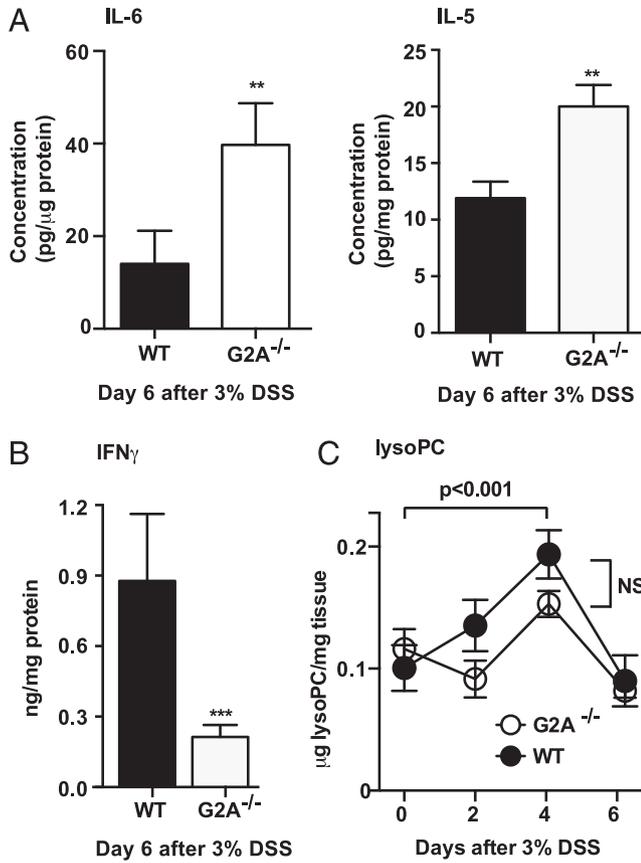
FIGURE 3. Loss of G2A receptor signaling results in altered cytokine production. IL-6, IL-5 (**A**), and IFN-γ (**B**) were among cytokines measured in homogenates from a 1-cm section of the distal colon by MesoScale Discovery Platform 6 d after administration of 3% DSS. Data represent mean ± SEM, $n = 10$. **$p < 0.01$, ***$p < 0.001$ versus WT. (**C**) LysoPC was quantified by liquid chromatography–tandem mass spectrometry in whole colon tissue over a time course of DSS colitis and showed a significant increase 4 d after administration of DSS. No difference was detected between the genotypes. Data represent mean ± SEM; $n = 6$.

Proinflammatory Ly6C^{hi}MHCII$^-$ monocytes are initially recruited from the blood to the tissues and have been shown to make TNF-α in DSS colitis, and over time, they begin to lose Ly6C expression and gain MHCII expression. These Ly6C^{int}MHCII$^+$ monocytes acquire anti-inflammatory features, as they have been shown to produce IL-10 (26, 27). In the G2A$^{-/-}$ mice, the number of proinflammatory monocytes (Ly6C^{hi}MHCII$^-$) was significantly higher by day 6 of DSS-induced colitis relative to WT (Fig. 4A). The number of monocytes staining for intracellular TNF-α were also significantly more numerous in the G2A$^{-/-}$ mice (Fig. 4B). In contrast, numbers of Ly6C^{int}MHCII$^+$ monocytes were no different between the genotypes. We were unable to identify IL-10 staining in monocytes of either genotype, attesting to the difficulty of intracellular staining for this cytokine, and, as noted above, no differences between genotypes were observed in levels of IL-10 measured in colonic tissue.

Proinflammatory monocytes are thought to contribute to host/biome responses and injury in DSS-induced colitis (24, 25). For example, both the CCR2$^{-/-}$ mice and mice in which monocytes have been depleted show improvement in various endpoints in DSS colitis (27, 29). As such, the potential role of proinflammatory monocytes in driving the excess inflammation seen in the G2A$^{-/-}$ mice was assessed using a monocyte-depleting Ab. As shown in Fig. 5A, prior treatment with the anti-CCR2 (MC-21) Ab efficiently depleted monocytes from both genotypes regardless of
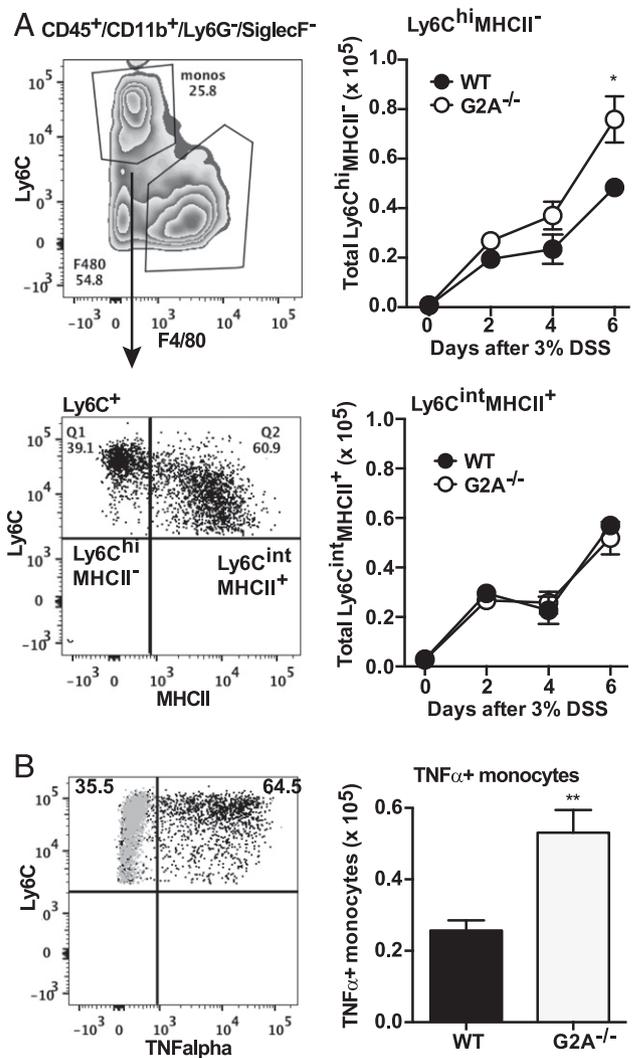
FIGURE 4. G2A$^{-/-}$ mice have more TNF-α$^+$ proinflammatory monocytes during DSS-induced colitis than WT. (**A**) Representative flow cytometry plot demonstrating gating strategy to separate Ly6C^{hi}MHCII$^-$ from Ly6C^{int}MHCII$^+$ monocytes (left). Total Ly6C^{hi}MHCII$^-$ and Ly6C^{int} MHCII$^+$ monocytes were determined by multiplying the percentage by the total number of monocytes from Fig. 2 (right). (**B**) Representative flow plot demonstrating intracellular TNF-α staining in the Ly6C-positive monocytes (left). Gray dots are isotype Ab controls. Total numbers of TNF-α$^+$ monocytes (right) were determined by multiplying the percentage of TNF-α$^+$ cells by the total number of monocytes from Fig. 2. Data represent mean ± SEM, $n = 10$. *$p < 0.05$, **$p < 0.01$ compared with WT.

phenotype. With monocyte depletion, the exacerbated disease activity and colon shortening in the G2A$^{-/-}$ mice were reduced to that seen in WT animals (Fig. 5B, 5C). Monocyte depletion in WT mice was associated with a trend toward lessened disease activity consistent with the findings by others (27, 30).

Notably, monocyte depletion abolished excess eosinophil numbers in the G2A$^{-/-}$ mice (Fig. 5D), indicating that monocytes can play a role in the accumulation of eosinophils, as reported previously (29). Eosinophil accumulation in colonic tissue of DSS-treated WT mice was unchanged with monocyte depletion. No changes were seen in neutrophil or lymphocyte numbers in either genotype with monocyte depletion.

Using an Ab directed to IL-5 (clone TRFK5), excess eosinophil numbers were depleted in the G2A$^{-/-}$ mice (Fig. 6A), and their exacerbated colon shortening and disease activity were significantly reduced to that of WT mice (Fig. 6B, 6C). Of note, eosinophils in
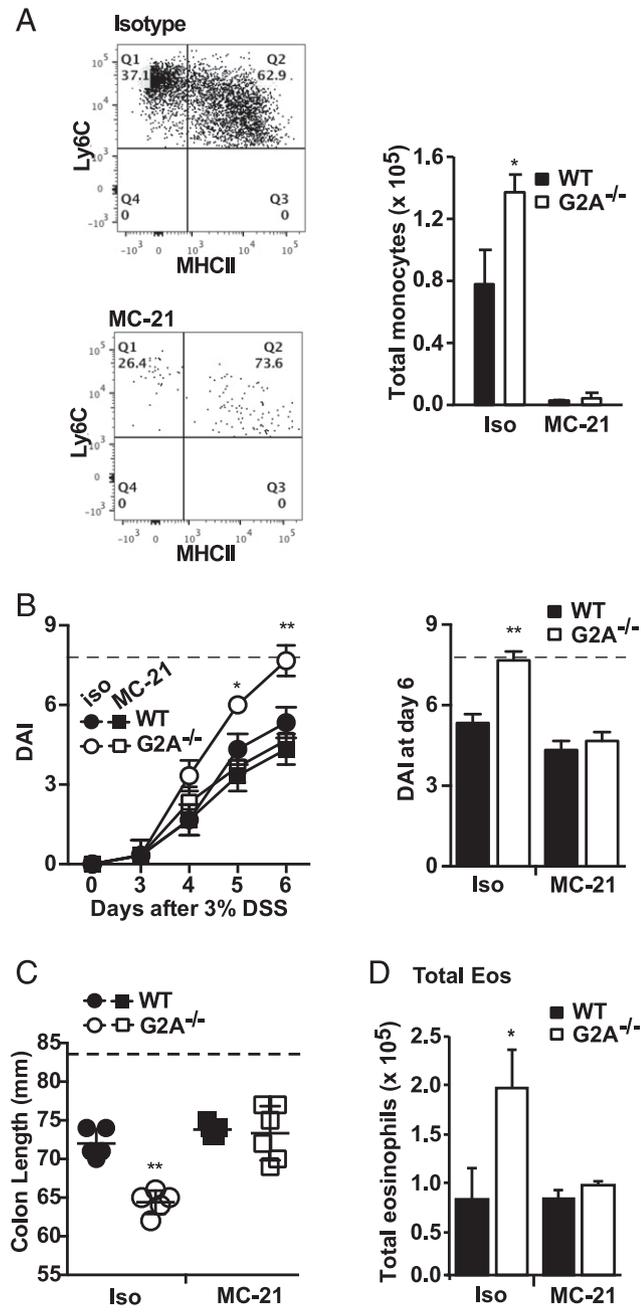
FIGURE 5. Depletion of monocytes limits disease severity in G2A$^{-/-}$ mice and reduces eosinophil numbers. Mice were treated with anti-CCR2 clone MC-21 (MC-21) or isotype Ab, as described in *Materials and Methods*. (**A**) Monocytes were depleted with MC-21. Left, Representative flow plot demonstrating efficient depletion of monocytes. Right, Total monocytes were significantly reduced in MC-21–treated animals (versus isotype treated) for both genotypes. (**B**) Disease activity index (DAI) was determined in MC-21– or isotype-treated mice over the time course of DSS exposure (left) and in an expanded representation for day 6 of DSS exposure (right). Dotted line indicates maximum DAI score. (**C**) Colon length was determined at day 6 following administration of DSS in MC-21– and isotype-treated animals. Dotted line represents colon length of water control animals. (**D**) Total numbers of eosinophils were determined with and without monocyte depletion with MC-21. Data represent mean ± SEM, $n = 10$. *$p < 0.05$, **$p < 0.01$ compared with WT isotype, WT MC-21, and G2A$^{-/-}$ MC-21.

WT mice were also reduced following anti–IL-5 Ab administration. However, in WT mice, colon shortening was worsened, and their disease activity was exacerbated, consistent with our previously

published data (31). Thus, subpopulations of eosinophils clearly play differing roles in DSS-induced colitis depending on genotype, mediating the worsened colitis in G2A$^{-/-}$ mice, whereas ameliorating colitis in WT (see *Discussion*).

The role of IFN-γ production in G2A$^{-/-}$ disease activity

IFN-γ production in colitis is thought to come from several lymphocyte populations (32, 33). Given the lower levels measured in inflamed colonic tissues of the G2A$^{-/-}$ mice (Fig. 3), possibly related to the reduced numbers of CD4 lymphocytes recruited to the colons of these mice (Fig. 2), we further investigated the role of IFN-γ. First, a time course of *Ifng* gene expression in whole colon tissue was assessed. *Ifnγ* mRNA in colonic tissues increased in WT mice by day 4 and was significantly elevated over baseline by day 6 (Fig. 7A). This increase was not evident in G2A$^{-/-}$ mice. The differences in the levels of IFN-γ in inflamed colons between the two genotypes (Fig. 3) were also evident in sera (Fig. 7B).

Next, we assessed stimulated production of IFN-γ from colonic digest cells. Cells (10^6) from DSS day 6 colon digests were cultured in media and stimulated with PMA and ionomycin for 4 h, and IFN-γ was assessed in the supernatants by ELISA. As shown,
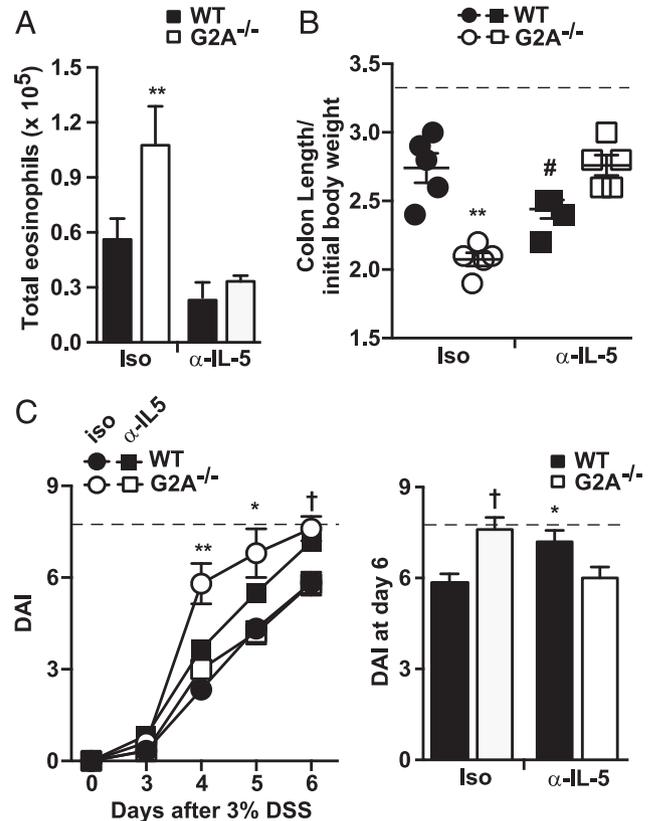
FIGURE 6. Treatment with anti–IL-5 (α-IL-5) reduces eosinophil numbers and disease severity in G2A$^{-/-}$ mice. Mice were treated with anti–IL-5 clone TRFK5 or isotype control Ab, as described in *Materials and Methods*. (**A**) Total eosinophils at day 6 were determined as described in Fig. 2. (**B**) Colon length normalized to initial body weight and (**C**) disease activity (DAI) determined over the time course of DSS exposure (left) and in an expanded representation for day 6 after DSS exposure (right). Dotted line represents colon length per initial body weight from water control animals (B) or maximum DAI score (C). Data represent mean ± SEM, $n = 10$. **$p < 0.01$ compared with WT isotype, WT anti–IL-5, and G2A$^{-/-}$ anti–IL-5, *$p < 0.05$ compared with G2A$^{-/-}$ anti–IL-5 or WT isotype, #$p < 0.05$ compared with WT isotype, G2A$^{-/-}$ isotype, and G2A$^{-/-}$ anti–IL-5, †$p < 0.01$ compared with WT isotype or G2A$^{-/-}$ anti–IL-5.
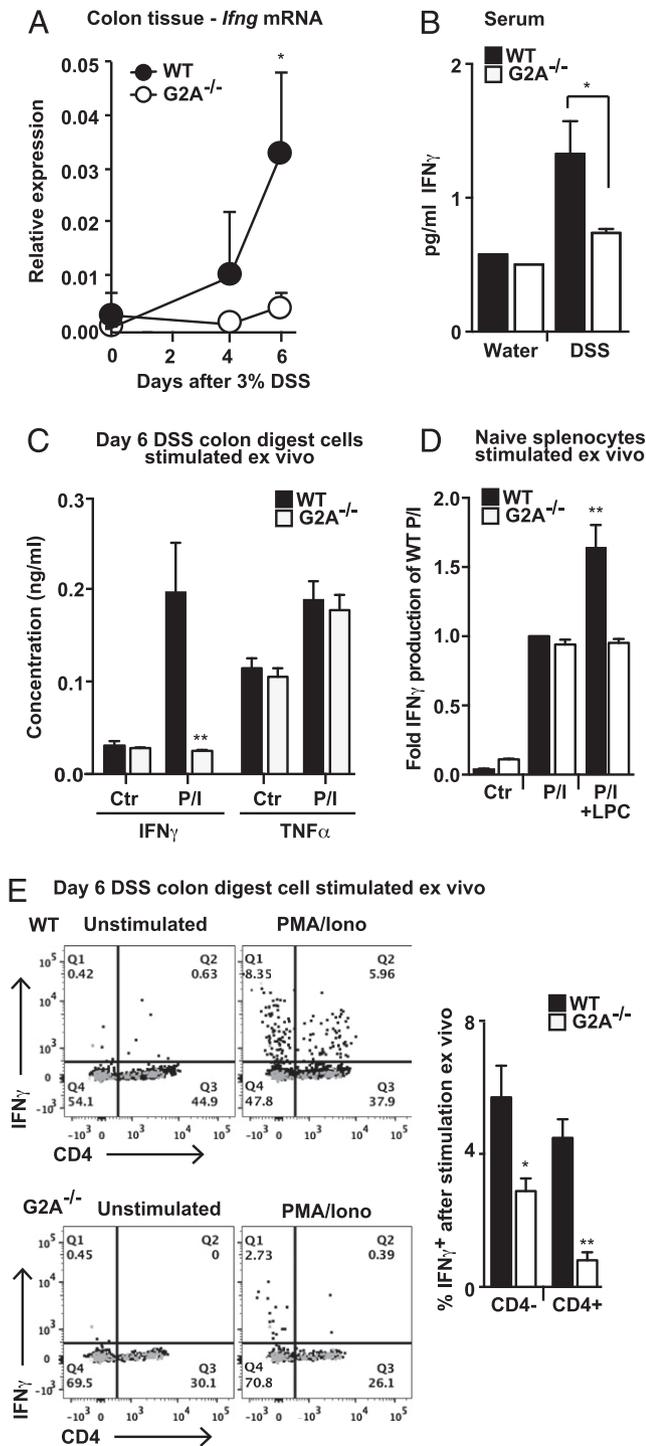
FIGURE 7. IFN-γ production is deficient in colon tissues and stimulated colonic lymphocytes from G2A$^{-/-}$ mice. (**A**) *Ifnγ* gene expression was determined by quantitative PCR from sections of distal colon over the time course of DSS-induced colitis. Data represent mean ± SEM, *n* = 10. *$p <$ 0.05 compared with G2A$^{-/-}$. (**B**) Serum was collected from whole blood from naive mice or at day 6 after administration of DSS, and IFN-γ concentration was determined as described in Fig. 3. Data represent mean ± SEM, *n* = 6–8. *$p <$ 0.05. (**C**) IFN-γ and TNF-α were measured by ELISA in cell-free supernatants following stimulation of cells from digested colons with PMA and ionomycin (P/I) for 4 h. Data represent mean ± SEM, *n* = 10. **$p <$ 0.01 compared with stimulated WT. (**D**) IFN-γ was measured in cell-free supernatants following stimulation of splenocytes from naive animals, as described in (C), in the presence or absence of 10 μM lysoPC (LPC). Data are displayed as fold of stimulated WT and represent mean ± SEM, *n* = 4–6. **$p <$ 0.01 compared with stimulated WT, stimulated G2A$^{-/-}$, and stimulated G2A$^{-/-}$ + LPC.

IFN-γ was profoundly deficient in culture supernatants from G2A$^{-/-}$ mice in comparison with WT mice (Fig. 7C), whereas stimulated TNF-α levels were not different between the genotypes. By contrast, PMA/ionomycin-stimulated spleen cells from naive G2A$^{-/-}$ and WT mice produced similar amounts of IFN-γ (Fig. 7D), showing that the ability to produce IFN-γ was not generally deficient in the G2A$^{-/-}$ animals. However, as hypothesized, only WT and not G2A$^{-/-}$ splenocytes made additional IFN-γ in response to lysoPC treatment. To better define potential sources of IFN-γ in the inflamed colons, colon digest cells were then stimulated as above in the presence of brefeldin A, stained for CD4 and intracellular IFN-γ, and analyzed by flow cytometry. Under these conditions, intracellular IFN-γ was evident in a proportion of stimulated CD4$^+$ and CD4$^-$ lymphocytes (Fig. 7E). When expressed as a percentage of total lymphocytes for each genotype, fewer were positive for IFN-γ in the G2A$^{-/-}$ animals than in WT (Fig. 7E). Thus, it appears likely that WT lymphocytes, most notably CD4$^+$ T cells, but also CD4$^-$ lymphocytes, are recruited to injured colons, and are primed/stimulated in a G2A-dependent manner for enhanced IFN-γ production. In the absence of G2A signaling, fewer numbers of CD4$^+$ lymphocytes are recruited during colitis, and these lymphocytes, as well as recruited CD4$^-$ lymphocytes, are deficient in their production of IFN-γ.

Ly6C^{int}MHCII$^+$ monocytes, in some settings, have been shown to bear an IFN-γ response signature (34, 35). We hypothesized that deficient IFN-γ in the colon of the G2A$^{-/-}$ mice might contribute to a blockade or delay in the transition of Ly6C^{hi} MHCII$^-$ proinflammatory monocytes to Ly6C^{int}MHCII$^+$ anti-inflammatory monocytes. To address this, G2A$^{-/-}$ mice were treated with IFN-γ (5 μg) on days 3 and 5 of DSS exposure with harvest of the animals at day 6. Following IFN-γ treatment, the total numbers of monocytes in the colons of G2A$^{-/-}$ were unchanged and remained elevated compared with WT colons (Fig. 8A). However, following IFN-γ treatment, the proportion of monocytes that were Ly6C^{hi}MHCII$^-$ was significantly lower, and the Ly6C^{int}MHCII$^+$ significantly greater in G2A$^{-/-}$ mice (Fig. 8A, Supplemental Fig. 2A). In support of the hypothesis that transition to Ly6C^{int}MHCII$^+$ is associated with a less inflammatory program, the number of monocytes staining positive for intracellular TNF-α was also reduced. Colon tissue IL-6 appeared to be reduced following IFN-γ treatment of G2A$^{-/-}$ mice, although the difference did not reach significance (Fig. 8B). Colon tissue IL-10 was no different (data not shown). IL-5 in colon tissues was significantly reduced following IFN-γ treatment, and, accordingly, eosinophil numbers were reduced to that seen in WT colon tissues (Fig. 8C).

Importantly, the exacerbated colitis in the G2A$^{-/-}$ mice was significantly ameliorated with IFN-γ treatment (Fig. 8D). Disease activity, colon lengths, and histology were all improved in G2A$^{-/-}$ mice with measures of each being similar to those seen in the WT mice, as well as substantially mimicking the effects of monocyte and eosinophil depletion (Figs. 5, 6). Identical treatment of WT mice with IFN-γ resulted in minimal reductions in disease

(**E**) Intracellular IFN-γ staining in control and stimulated (PMA and ionomycin for 4 h) colon digest cells from day 6 DSS in the presence of brefeldin A. Representative flow plots demonstrating intracellular IFN-γ staining in control or stimulated B220$^-$SSC^{lo} CD4$^+$ and CD4$^-$ lymphocytes (left). Gray dots are stained with isotype control Ab. The percentage of stimulated B220$^-$CD4$^-$ or B220$^-$CD4$^+$ lymphocytes staining positive for IFN-γ in WT or G2A$^{-/-}$ mice is shown (right). Data represent mean ± SEM, *n* = 10. *$p <$ 0.05, **$p <$ 0.01 compared with WT.

FIGURE 8. Provision of IFN-γ to G2A$^{-/-}$ mice enhances anti-inflammatory monocyte programming, reduces IL-5 and eosinophils, and limits disease severity. G2A$^{-/-}$ mice were treated with 5 μg IFN-γ on days 3 and 5 after administration of 3% DSS and harvested at day 6. (**A**) Total monocytes, Ly6C^{hi}MHCII$^-$ monocytes and Ly6C^{int}MHCII$^+$ monocytes, and TNF-α$^+$ monocytes were determined, as described in Figs. 2 and 4. Data represent mean ± SEM; $n = 15$, *$p < 0.05$, **$p < 0.01$. (**B**) IL-6 concentration in a distal section of colon tissue was determined, as described in Fig. 3. Data represent mean ± SEM; $n = 6$, *$p < 0.05$. (**C**) IL-5 concentration was determined, as described in (B), and total eosinophil numbers were determined, as described in Fig. 2. Data represent mean ± SEM, $n = 15$. *$p < 0.05$, **$p < 0.01$. (**D**) Disease activity (DAI) (left), colon length (middle), and total histologic index (right) were determined, as described in Fig. 1. Dotted line represents maximum DAI score (left) or colon length of water control animals (middle). Lower, Representative histologic images of WT, G2A$^{-/-}$, or IFN-γ–treated G2A$^{-/-}$ mice. Data represent mean ± SEM, $n = 15$. *$p < 0.05$ compared with WT, **$p < 0.01$ compared with WT and G2A$^{-/-}$ IFN-γ, #$p < 0.01$ compared with G2A$^{-/-}$.
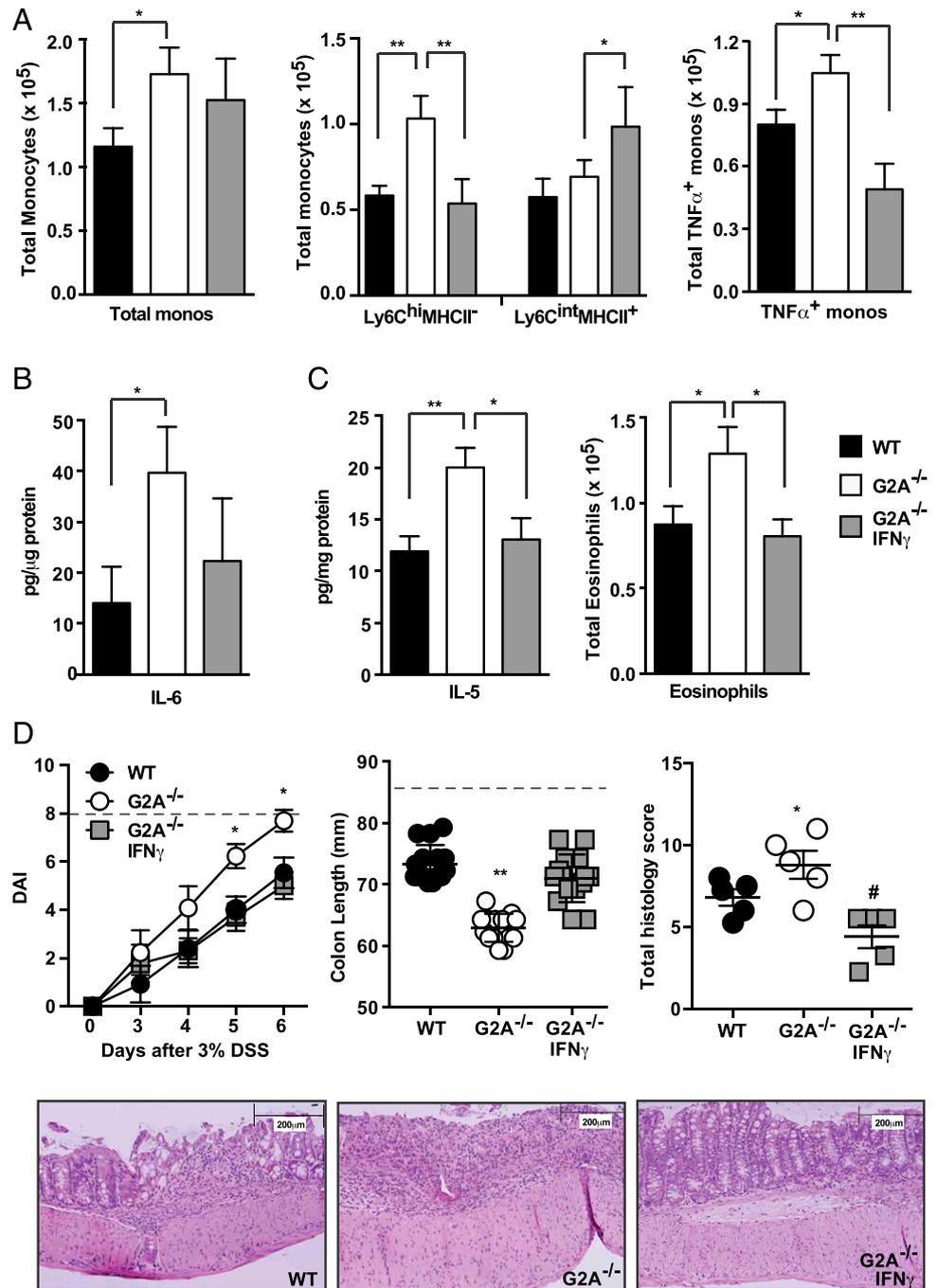
activity, colon shortening, and cellular infiltration, suggesting optimal effects from endogenously produced IFN-γ (Supplemental Fig. 2B–D).

Discussion

Production of lysoPC accompanies epithelial cell injury in the airway (9, 10) and the intestine (11, 12) and results in a variety of proinflammatory actions mediated through the G protein–coupled receptor G2A present on recruited inflammatory cells (8). Although our investigation of colitis in G2A$^{-/-}$ mice began with the hypothesis that loss of this receptor would be therapeutic, this hypothesis is refuted with unequivocal evidence that the G protein–coupled receptor serves to dampen inflammation in this model. Key elements were identified in this investigation, as follows: excess inflammation and disease activity in the G2A$^{-/-}$ mice were attributable to activities of proinflammatory subpopulations of

monocytes and eosinophils, and, surprisingly, injury from these effector cells was ultimately the result of diminished production of IFN-γ.

IFN-γ is elevated in colonic tissues in human inflammatory bowel disease as well as in animal colitis models (4–7). IFN-γ is generally thought of as a quintessential proinflammatory cytokine required in many instances for innate and Th1 adaptive immunity, although its effects are protean. Genetic ablation of IFN-γ or its neutralization has been shown by some (32, 36) but not other investigators (37) to ameliorate disease severity in the DSS model. These mixed findings and our data, in this work, may help to explain the lack of therapeutic success of blocking the action of IFN-γ in human IBD (38).

The sources of IFN-γ in DSS colitis are thought to be various lymphocyte populations, including both CD4 and CD8 cells after exposure to inflamed colonic epithelial cells (32). We

have shown deficient recruitment of CD4 lymphocytes to inflamed colons in the G2A$^{-/-}$ mice, and that recruited lymphocyte populations, both CD4$^+$ and CD4$^-$, seem to produce less IFN-γ in response to stimulation than lymphocytes of WT mice (Fig. 7). The most likely explanation is that the G2A$^{-/-}$ lymphocytes cannot be primed/activated for enhanced production of IFN-γ by lysoPC (18). In this regard, we note that the G2A receptor can also respond to other signals aside from lysoPC, for example, lysoPS (39). We measured lysoPS and found it present at very low levels in both genotypes for most of the course of colitis (data not shown). Although we cannot rule out a contribution in WT mice from lysoPS/G2A anti-inflammatory modulation of monocyte programming (23), to our knowledge only lysoPC/G2A signaling has been associated with IFN-γ production by lymphocytes (16, 18). Of note, in recent studies of DSS colitis and ulcerative colitis in humans, it was shown that lysoPC ultimately declines with disease chronicity (12, 40), and, given our findings, we hypothesize this may result in deficient G2A signaling and the resulting inflammatory events demonstrated in this work.

Despite the defined effect of G2A signaling on dampening the degree of colonic inflammation and disease in this model, a key future question is the specific cell target(s) for the G2A effect and the proposed effect of lysoPC stimulation. However, even in the absence of isolating G2A deficiency on one cell type or another, the approach taken in this study allowed us to elucidate specific roles and a hierarchy for the key effector cells/mediators. First, depletion of either eosinophils or monocytes using depleting Abs, or the institution of IFN-γ treatment, all resulted in nearly identical amelioration of the enhanced disease activity, histological changes, and colon shortening in the G2A$^{-/-}$ mice (comparing Figs. 5, 6, and 8). Thus, a common pathway is suggested. Further support for this comes from the observation that both monocyte depletion and IFN-γ treatment resulted in elimination of excess eosinophil numbers in the G2A-deficient mice, whereas eosinophil depletion in these mice had no obvious effect on these other key elements. This allows us to position eosinophils as a candidate final effector cell responsible for excess colonic injury in the G2A$^{-/-}$ mice. An important observation is that, whereas depletion of excess eosinophils in the G2A$^{-/-}$ mice was ameliorative of heightened inflammation and disease activity, depletion of eosinophils in WT animals exacerbated injury. This latter finding has been recently published and is attributed to deficient eosinophil 15-lipoxygenase production of protectin D1 (31). Furthermore, intestinal eosinophils are present in the colon in homeostasis in both genotypes and not fully amenable to this depletion strategy. These data highlight the observations that eosinophils can play many immunomodulating roles differing in intestinal homeostasis and disease states (41, 42). Clearly, their activation status, numbers, and location are likely of great importance to such heterogeneity and the different roles that they play, and the potential role of G2A on eosinophils, themselves, are all key areas for further investigation.

Perhaps the most surprising finding in this investigation of colitis in the G2A$^{-/-}$ mice was the prominent role of IFN-γ in the anti-inflammatory programming of recruited monocytes. Several groups have shown that monocytes recruited to the inflamed colon in the DSS model exhibit marked heterogeneity (26, 27). They are known to progress from Ly6C^{hi} MHCII$^-$ TNF-α–producing monocytes through loss of Ly6C and gain of MHCII in association with IL-10 production (26, 27). We have shown that treatment with IFN-γ, although not affecting overall numbers of monocytes in G2A$^{-/-}$ mice, appeared to enhance the acquisition of MHCII on monocytes in the G2A$^{-/-}$ mice (Fig. 8A, Supplemental Fig. 2A), an effect consistent with actions of IFN-γ in other contexts (33, 43). We were unable to replicate enhanced intracellular

staining of IL-10 in the resulting Ly6C^{int}MHCII$^+$ monocytes in either WT or G2A$^{-/-}$ mice (data not shown), and levels of IL-10, known to be produced by other sources in colitis (44–46), were not different between G2A$^{-/-}$ and WT colitic mice. Importantly, the enhanced transition of monocytes to Ly6C^{int}MHCII$^+$ driven by IFN-γ was accompanied by diminished numbers of TNF-α^+ monocytes (Fig. 8A). TNF-α clearly plays an important role in the DSS model (47, 48) and human IBD, where it is a proven therapeutic target (49–51). This anti-inflammatory activity of IFN-γ on monocytes adds to accumulating evidence that IFN-γ may display inflammation-mitigating properties in mucosal inflammation models (52). IFN-γ has, for example, been shown to mediate anti-inflammatory properties through induction of IDO 1 (53), regulation of the methylation response (54), and induction of epithelial IL-10Rs (20) supportive of healing responses by the epithelium. We also note that anti-inflammatory activities of IFN-γ on monocytes have also recently been described in the context of gastrointestinal infection (43).

In summary, the G protein–coupled receptor G2A appears to be important in limiting disease severity in this model of acute colitis driven by insult to the epithelium and propagated by innate host response to microflora. G2A signaling does so through a complex interaction of IFN-γ production, monocyte programming, and eosinophil-induced injury. Investigation of its roles in chronic intestinal inflammation, other models of IBD, and other models of epithelial insult, for example, airways, is likely to provide new mechanistic insights and possible therapeutic targets following mucosal injury.

Disclosures

The authors have no financial conflicts of interest.

References

1. Xavier, R. J., and D. K. Podolsky. 2007. Unravelling the pathogenesis of inflammatory bowel disease. *Nature* 448: 427–434.
2. Peters, C. P., J. M. Mjosberg, J. H. Bernink, and H. Spits. 2016. Innate lymphoid cells in inflammatory bowel diseases. *Immunol. Lett.* 172: 124–131.
3. Chassaing, B., J. D. Aitken, M. Malleshappa, and M. Vijay-Kumar. 2014. Dextran sulfate sodium (DSS)-induced colitis in mice. *Curr. Prot. Immunol.* 104: Unit 15.25.
4. Perše, M., and A. Cerar. 2012. Dextran sodium sulphate colitis mouse model: traps and tricks. *J. Biomed. Biotechnol.* DOI: 10.1155/2012/718617.
5. Alex, P., N. C. Zachos, T. Nguyen, L. Gonzales, T. E. Chen, L. S. Conklin, M. Centola, and X. Li. 2009. Distinct cytokine patterns identified from multiplex profiles of murine DSS and TNBS-induced colitis. *Inflamm. Bowel Dis.* 15: 341–352.
6. Egger, B., M. Bajaj-Elliott, T. T. MacDonald, R. Inglin, V. E. Eysselein, and M. W. Büchler. 2000. Characterisation of acute murine dextran sodium sulphate colitis: cytokine profile and dose dependency. *Digestion* 62: 240–248.
7. Yan, Y., V. Kolachala, G. Dalmasso, H. Nguyen, H. Laroui, S. V. Sitaraman, and D. Merlin. 2009. Temporal and spatial analysis of clinical and molecular parameters in dextran sodium sulfate induced colitis. *PLoS One* 4: e6073.
8. Kabarowski, J. H. 2009. G2A and LPC: regulatory functions in immunity. *Prostaglandins Other Lipid Mediat.* 89: 73–81.
9. Yoder, M., Y. Zhuge, Y. Yuan, O. Holian, S. Kuo, R. van Breemen, L. L. Thomas, and H. Lum. 2014. Bioactive lysophosphatidylcholine 16:0 and 18:0 are elevated in lungs of asthmatic subjects. *Allergy Asthma Immunol. Res.* 6: 61–65.
10. Zhuge, Y., Y. Yuan, R. van Breemen, O. Degrand, O. Holian, M. Yoder, and H. Lum. 2014. Stimulated bronchial epithelial cells release bioactive lysophosphatidylcholine 16:0, 18:0, and 18:1. *Allergy Asthma Immunol. Res.* 6: 66–74.
11. Braun, A., I. Treede, D. Gotthardt, A. Tietje, A. Zahn, R. Ruhwald, U. Schoenfeld, T. Welsch, P. Kienle, G. Erben, et al. 2009. Alterations of phospholipid concentration and species composition of the intestinal mucus barrier in ulcerative colitis: a clue to pathogenesis. *Inflamm. Bowel Dis.* 15: 1705–1720.
12. Ehehalt, R., J. Wagenblast, G. Erben, W. D. Lehmann, U. Hinz, U. Merle, and W. Stremmel. 2004. Phosphatidylcholine and lysophosphatidylcholine in intestinal mucus of ulcerative colitis patients: a quantitative approach by nanoElectrospray-tandem mass spectrometry. *Scand. J. Gastroenterol.* 39: 737–742.

13. Lauber, K., E. Bohn, S. M. Kröber, Y. J. Xiao, S. G. Blumenthal, R. K. Lindemann, P. Marini, C. Wiedig, A. Zobywalski, S. Baksh, et al. 2003. Apoptotic cells induce migration of phagocytes via caspase-3-mediated release of a lipid attraction signal. *Cell* 113: 717–730.

14. Peter, C., M. Waibel, C. G. Radu, L. V. Yang, O. N. Witte, K. Schulze-Osthoff, S. Wesselborg, and K. Lauber. 2008. Migration to apoptotic "find-me" signals is mediated via the phagocyte receptor G2A. *J. Biol. Chem.* 283: 5296–5305.

15. Radu, C. G., L. V. Yang, M. Riedinger, M. Au, and O. N. Witte. 2004. T cell chemotaxis to lysophosphatidylcholine through the G2A receptor. *Proc. Natl. Acad. Sci. USA* 101: 245–250.

16. Yan, J. J., J. S. Jung, J. E. Lee, J. Lee, S. O. Huh, H. S. Kim, K. C. Jung, J. Y. Cho, J. S. Nam, H. W. Suh, et al. 2004. Therapeutic effects of lysophosphatidylcholine in experimental sepsis. *Nat. Med.* 10: 161–167.

17. Nishioka, H., H. Horiuchi, H. Arai, and T. Kita. 1998. Lysophosphatidylcholine generates superoxide anions through activation of phosphatidylinositol 3-kinase in human neutrophils. *FEBS Lett.* 441: 63–66.

18. Nishi, E., N. Kume, Y. Ueno, H. Ochi, H. Moriwaki, and T. Kita. 1998. Lysophosphatidylcholine enhances cytokine-induced interferon gamma expression in human T lymphocytes. *Circ. Res.* 83: 508–515.

19. Cooper, H. S., S. N. Murthy, R. S. Shah, and D. J. Sedergran. 1993. Clinicopathologic study of dextran sulfate sodium experimental murine colitis. *Lab. Invest.* 69: 238–249.

20. Kominsky, D. J., E. L. Campbell, S. F. Ehrentraut, K. E. Wilson, C. J. Kelly, L. E. Glover, C. B. Collins, A. J. Bayless, B. Saeedi, E. Dobrinskikh, et al. 2014. IFN-γ-mediated induction of an apical IL-10 receptor on polarized intestinal epithelia. *J. Immunol.* 192: 1267–1276.

21. Bligh, E. G., and W. J. Dyer. 1959. A rapid method of total lipid extraction and purification. *Can. J. Biochem. Physiol.* 37: 911–917.

22. Frasch, S. C., K. Z. Berry, R. Fernandez-Boyanapalli, H. S. Jin, C. Leslie, P. M. Henson, R. C. Murphy, and D. L. Bratton. 2008. NADPH oxidase-dependent generation of lysophosphatidylserine enhances clearance of activated and dying neutrophils via G2A. *J. Biol. Chem.* 283: 33736–33749.

23. Frasch, S. C., R. F. Fernandez-Boyanapalli, K. A. Berry, R. C. Murphy, C. C. Leslie, J. A. Nick, P. M. Henson, and D. L. Bratton. 2013. Neutrophils regulate tissue neutrophilia in inflammation via the oxidant-modified lipid lysophosphatidylserine. *J. Biol. Chem.* 288: 4583–4593.

24. Bain, C. C., and A. M. Mowat. 2014. The monocyte-macrophage axis in the intestine. *Cell. Immunol.* 291: 41–48.

25. Platt, A. M., C. C. Bain, Y. Bordon, D. P. Sester, and A. M. Mowat. 2010. An independent subset of TLR expressing CCR2-dependent macrophages promotes colonic inflammation. *J. Immunol.* 184: 6843–6854.

26. Bain, C. C., C. L. Scott, H. Uronen-Hansson, S. Gudjonsson, O. Jansson, O. Grip, M. Guilliams, B. Malissen, W. W. Agace, and A. M. Mowat. 2013. Resident and pro-inflammatory macrophages in the colon represent alternative context-dependent fates of the same Ly6Chi monocyte precursors. *Mucosal Immunol.* 6: 498–510.

27. Zigmond, E., C. Varol, J. Farache, E. Elmaliah, A. T. Satpathy, G. Friedlander, M. Mack, N. Shpigel, I. G. Boneca, K. M. Murphy, et al. 2012. Ly6C hi monocytes in the inflamed colon give rise to proinflammatory effector cells and migratory antigen-presenting cells. *Immunity* 37: 1076–1090.

28. Kiesler, P., I. J. Fuss, and W. Strober. 2015. Experimental models of inflammatory bowel diseases. *Cell. Mol. Gastroenterol. Hepatol.* 1: 154-170.

29. Waddell, A., R. Ahrens, K. Steinbrecher, B. Donovan, M. E. Rothenberg, A. Munitz, and S. P. Hogan. 2011. Colonic eosinophilic inflammation in experimental colitis is mediated by Ly6C(high) CCR2(+) inflammatory monocyte/macrophage-derived CCL11. *J. Immunol.* 186: 5993–6003.

30. Moshkovits, I., H. Reichman, D. Karo-Atar, P. Rozenberg, E. Zigmond, Y. Haberman, N. Ben Baruch-Morgenstern, M. Lampinen, M. Carlson, M. Itan, et al. 2016. A key requirement for CD300f in innate immune responses of eosinophils in colitis. Mucosal Immunol. *DOI: 10.1038/mi.2016.37*.

31. Masterson, J. C., E. N. McNamee, S. A. Fillon, L. Hosford, R. Harris, S. D. Fernando, P. Jedlicka, R. Iwamoto, E. Jacobsen, C. Protheroe, et al. 2015. Eosinophil-mediated signalling attenuates inflammatory responses in experimental colitis. *Gut* 64: 1236–1247.

32. Nava, P., S. Koch, M. G. Laukoetter, W. Y. Lee, K. Kolegraff, C. T. Capaldo, N. Beeman, C. Addis, K. Gerner-Smidt, I. Neumaier, et al. 2010. Interferon-gamma regulates intestinal epithelial homeostasis through converging beta-catenin signaling pathways. *Immunity* 32: 392–402.

33. Thelemann, C., R. O. Eren, M. Coutaz, J. Brasseit, H. Bouzourene, M. Rosa, A. Duval, C. Lavanchy, V. Mack, C. Mueller, et al. 2014. Interferon-γ induces expression of MHC class II on intestinal epithelial cells and protects mice from colitis. *PLoS One* 9: e86844.

34. Jakubzick, C., E. L. Gautier, S. L. Gibbings, D. K. Sojka, A. Schlitzer, T. E. Johnson, S. Ivanov, Q. Duan, S. Bala, T. Condon, et al. 2013. Minimal differentiation of classical monocytes as they survey steady-state tissues and transport antigen to lymph nodes. *Immunity* 39: 599–610.

35. Rivollier, A., J. He, A. Kole, V. Valatas, and B. L. Kelsall. 2012. Inflammation switches the differentiation program of Ly6Chi monocytes from antiinflammatory macrophages to inflammatory dendritic cells in the colon. *J. Exp. Med.* 209: 139–155.

36. Ito, R., M. Shin-Ya, T. Kishida, A. Urano, R. Takada, J. Sakagami, J. Imanishi, M. Kita, Y. Ueda, Y. Iwakura, et al. 2006. Interferon-gamma is causatively involved in experimental inflammatory bowel disease in mice. *Clin. Exp. Immunol.* 146: 330–338.

37. Sheikh, S. Z., K. Matsuoka, T. Kobayashi, F. Li, T. Rubinas, and S. E. Plevy. 2010. Cutting edge: IFN-gamma is a negative regulator of IL-23 in murine macrophages and experimental colitis. *J. Immunol.* 184: 4069–4073.

38. Cottone, M., A. Orlando, and S. Renna. 2010. Investigational agents for Crohn's disease. *Expert Opin. Investig. Drugs* 19: 1147–1159.

39. Frasch, S. C., K. Zemski-Berry, R. C. Murphy, N. Borregaard, P. M. Henson, and D. L. Bratton. 2007. Lysophospholipids of different classes mobilize neutrophil secretory vesicles and induce redundant signaling through G2A. *J. Immunol.* 178: 6540–6548.

40. Bauer, J., G. Liebisch, C. Hofmann, C. Huy, G. Schmitz, F. Obermeier, and J. Bock. 2009. Lipid alterations in experimental murine colitis: role of ceramide and imipramine for matrix metalloproteinase-1 expression. *PLoS One* 4: e7197.

41. Hogan, S. P., A. Waddell, and P. C. Fulkerson. 2013. Eosinophils in infection and intestinal immunity. *Curr. Opin. Gastroenterol.* 29: 7–14.

42. Woodruff, S. A., J. C. Masterson, S. Fillon, Z. D. Robinson, and G. T. Furuta. 2011. Role of eosinophils in inflammatory bowel and gastrointestinal diseases. *J. Pediatr. Gastroenterol. Nutr.* 52: 650–661.

43. Askenase, M. H., S. J. Han, A. L. Byrd, D. Morais da Fonseca, N. Bouladoux, C. Wilhelm, J. E. Konkel, T. W. Hand, N. Lacerda-Queiroz, X. Z. Su, et al. 2015. Bone-marrow-resident NK cells prime monocytes for regulatory function during infection. *Immunity* 42: 1130–1142.

44. Shouval, D. S., A. Biswas, J. A. Goettel, K. McCann, E. Conaway, N. S. Redhu, I. D. Mascanfroni, Z. Al Adham, S. Lavoie, M. Ibourk, et al. 2014. Interleukin-10 receptor signaling in innate immune cells regulates mucosal immune tolerance and anti-inflammatory macrophage function. *Immunity* 40: 706–719.

45. Shouval, D. S., J. Ouahed, A. Biswas, J. A. Goettel, B. H. Horwitz, C. Klein, A. M. Muise, and S. B. Snapper. 2014. Interleukin 10 receptor signaling: master regulator of intestinal mucosal homeostasis in mice and humans. *Adv. Immunol.* 122: 177–210.

46. Zigmond, E., B. Bernshtein, G. Friedlander, C. R. Walker, S. Yona, K. W. Kim, O. Brenner, R. Krauthgamer, C. Varol, W. Müller, and S. Jung. 2014. Macrophage-restricted interleukin-10 receptor deficiency, but not IL-10 deficiency, causes severe spontaneous colitis. *Immunity* 40: 720–733.

47. Stillie, R., and A. W. Stadnyk. 2009. Role of TNF receptors, TNFR1 and TNFR2, in dextran sodium sulfate-induced colitis. *Inflamm. Bowel Dis.* 15: 1515–1525.

48. Wang, K., G. Han, Y. Dou, Y. Wang, G. Liu, R. Wang, H. Xiao, X. Li, C. Hou, B. Shen, et al. 2012. Opposite role of tumor necrosis factor receptors in dextran sulfate sodium-induced colitis in mice. *PLoS One* 7: e52924.

49. Bradley, J. R. 2008. TNF-mediated inflammatory disease. *J. Pathol.* 214: 149–160.

50. Peyrin-Biroulet, L. 2010. Anti-TNF therapy in inflammatory bowel diseases: a huge review. *Minerva Gastroenterol. Dietol.* 56: 233–243.

51. Sandborn, W. J., S. Hanauer, E. V. Loftus, Jr., W. J. Tremaine, S. Kane, R. Cohen, K. Hanson, T. Johnson, D. Schmitt, and R. Jeche. 2004. An open-label study of the human anti-TNF monoclonal antibody adalimumab in subjects with prior loss of response or intolerance to infliximab for Crohn's disease. *Am. J. Gastroenterol.* 99: 1984–1989.

52. Muzaki, A. R., P. Tetlak, J. Sheng, S. C. Loh, Y. A. Setiagani, M. Poidinger, F. Zolezzi, K. Karjalainen, and C. Ruedl. 2016. Intestinal CD103(+)CD11b(-) dendritic cells restrain colitis via IFN-γ-induced anti-inflammatory response in epithelial cells. *Mucosal Immunol.* 9: 336–351.

53. Gurtner, G. J., R. D. Newberry, S. R. Schloemann, K. G. McDonald, and W. F. Stenson. 2003. Inhibition of indoleamine 2,3-dioxygenase augments trinitrobenzene sulfonic acid colitis in mice. *Gastroenterology* 125: 1762–1773.

54. Kominsky, D. J., S. Keely, C. F. MacManus, L. E. Glover, M. Scully, C. B. Collins, B. E. Bowers, E. L. Campbell, and S. P. Colgan. 2011. An endogenously anti-inflammatory role for methylation in mucosal inflammation identified through metabolite profiling. *J. Immunol.* 186: 6505–6514.